Charmonium production at HERA

B.A. Kniehl[1] and V. Velizhanin[1,2]

[1]II. Institute for Theoretical Physics
Hamburg University

[2]Theory Division
Petersburg Nuclear Physics Institute

International Workshop on Heavy Quarkonium 2007,
17-20 October 2007, DESY Hamburg

Introduction

Models for charmonium production

The production of heavy quarkonium in high energy collisions provides an important tool to study the interplay between perturbative and nonperturbative QCD dynamics.

The creation of $Q\bar{Q}$ pair is a short-distance process and can be calculated in pQCD.

The non-perturbative transition from the $Q\bar{Q}$ pair to a physical quarkonium involves long-distance scales of the order of the quarkonium size.

Color Singlet Model:

E.L. Berger, D. Jones, Phys. Rev. D23 (1981) 1521; R. Baier, R. Ruckl, Phys. Lett. 102B (1981) 364.

- Factorization in perturbative short-distance part and nonperturbative long-distance part.
- $Q\bar{Q}$ pair must be in color singlet state and have the same $^{2S+1}L_J$ quantum numbers as heavy quarkonium H.
- IR divergences in P-wave.

Color Evaporation Model:

H. Fritzsch, Phys. Lett. B67 (1977) 217; F. Halzen, Phys. Lett. B69 (1977) 105; M. Gluck, J.F. Owens, E. Reya, Phys. Rev. D17 (1978) 2324.

Hard comover scattering:

P. Hoyer, S. Peigne, Phys. Rev. D59 (1999) 034011; N. Marchal, S. Peigne, P. Hoyer, Phys. Rev. D62 (2000) 114001.

Introduction

Models for charmonium production

The production of heavy quarkonium in high energy collisions provides an important tool to study the interplay between perturbative and nonperturbative QCD dynamics.

The creation of $Q\bar{Q}$ pair is a short-distance process and can be calculated in pQCD.

The non-perturbative transition from the $Q\bar{Q}$ pair to a physical quarkonium involves long-distance scales of the order of the quarkonium size.

Color Singlet Model:

E.L. Berger, D. Jones, Phys. Rev. D23 (1981) 1521; R. Baier, R. Ruckl, Phys. Lett. 102B (1981) 364.

- Factorization in perturbative short-distance part and nonperturbative long-distance part.
- $Q\bar{Q}$ pair must be in color singlet state and have the same $^{2S+1}L_J$ quantum numbers as heavy quarkonium H.
- IR divergences in P-wave.

Color Evaporation Model:

H. Fritzsch, Phys. Lett. B67 (1977) 217; F. Halzen, Phys. Lett. B69 (1977) 105; M. Gluck, J.F. Owens, E. Reya, Phys. Rev. D17 (1978) 2324.

Hard comover scattering:

P. Hoyer, S. Peigne, Phys. Rev. D59 (1999) 034011; N. Marchal, S. Peigne, P. Hoyer, Phys. Rev. D62 (2000) 114001.

Introduction

Models for charmonium production

The production of heavy quarkonium in high energy collisions provides an important tool to study the interplay between perturbative and nonperturbative QCD dynamics.

The creation of $Q\bar{Q}$ pair is a short-distance process and can be calculated in pQCD.

The non-perturbative transition from the $Q\bar{Q}$ pair to a physical quarkonium involves long-distance scales of the order of the quarkonium size.

Color Singlet Model:

E.L. Berger, D. Jones, Phys. Rev. D23 (1981) 1521; R. Baier, R. Ruckl, Phys. Lett. 102B (1981) 364.

- Factorization in perturbative short-distance part and nonperturbative long-distance part.
- $Q\bar{Q}$ pair must be in color singlet state and have the same ${}^{2S+1}L_J$ quantum numbers as heavy quarkonium H.
- IR divergences in P-wave.

Color Evaporation Model:

H. Fritzsch, Phys. Lett. B67 (1977) 217; F. Halzen, Phys. Lett. B69 (1977) 105; M. Gluck, J.F. Owens, E. Reya, Phys. Rev. D17 (1978) 2324.

Hard comover scattering:

P. Hoyer, S. Peigne, Phys. Rev. D59 (1999) 034011; N. Marchal, S. Peigne, P. Hoyer, Phys. Rev. D62 (2000) 114001.

Introduction

Models for charmonium production

The production of heavy quarkonium in high energy collisions provides an important tool to study the interplay between perturbative and nonperturbative QCD dynamics.

The creation of $Q\bar{Q}$ pair is a short-distance process and can be calculated in pQCD.

The non-perturbative transition from the $Q\bar{Q}$ pair to a physical quarkonium involves long-distance scales of the order of the quarkonium size.

Color Singlet Model:

E.L. Berger, D. Jones, Phys. Rev. D23 (1981) 1521; R. Baier, R. Ruckl, Phys. Lett. 102B (1981) 364.

- Factorization in perturbative short-distance part and nonperturbative long-distance part.
- $Q\bar{Q}$ pair must be in color singlet state and have the same ${}^{2S+1}L_J$ quantum numbers as heavy quarkonium H.
- IR divergences in P-wave.

Color Evaporation Model:

H. Fritzsch, Phys. Lett. B67 (1977) 217; F. Halzen, Phys. Lett. B69 (1977) 105; M. Gluck, J.F. Owens, E. Reya, Phys. Rev. D17 (1978) 2324.

Hard comover scattering:

P. Hoyer, S. Peigne, Phys. Rev. D59 (1999) 034011; N. Marchal, S. Peigne, P. Hoyer, Phys. Rev. D62 (2000) 114001.

Introduction

Models for charmonium production

NRQCD factorization formalism:

W. E. Caswell, G. P. Lepage, Phys. Lett. B167 (1986) 437; G.T. Bodwin, E. Braaten, G.P. Lepage, Phys. Rev. D51 (1995) 1125; D55 (1997) 5853 (E).

- Factorization in perturbative short-distance coeficients and long-distance matrix elements:

$$d\sigma(a + b \to H + X) = \sum_n d\hat{\sigma}(a + b \to Q\overline{Q}\,[n] + X)\,\langle \mathcal{O}^H\,[n]\rangle,$$

  where the sum includes all colour and angular momentum states of the $Q\overline{Q}$ pair, denoted collectively by $n = {}^{2S+1}L_J^{(c)}$.
- Long-distance matrix elements (free parameters) universal, relative sizes predicted by velocity scaling rules.
- Double expansion in α_s and υ.
- Renormalizable, predictive.

Introduction

Models for charmonium production

NRQCD factorization formalism:

W. E. Caswell, G. P. Lepage, Phys. Lett. B167 (1986) 437; G.T. Bodwin, E. Braaten, G.P. Lepage, Phys. Rev. D51 (1995) 1125; D55 (1997) 5853 (E).

- Factorization in perturbative short-distance coeficients and long-distance matrix elements:

$$d\sigma(a+b\to H+X)=\sum_n d\hat{\sigma}(a+b\to Q\overline{Q}\,[n]+X)\,\langle\mathcal{O}^H\,[n]\rangle,$$

  where the sum includes all colour and angular momentum states of the $Q\overline{Q}$ pair, denoted collectively by $n={}^{2S+1}L_J^{(c)}$.
- Long-distance matrix elements (free parameters) universal, relative sizes predicted by velocity scaling rules.
- Double expansion in α_s and v.
- Renormalizable, predictive.

Introduction

Models for charmonium production

NRQCD factorization formalism:

W. E. Caswell, G. P. Lepage, Phys. Lett. B167 (1986) 437; G.T. Bodwin, E. Braaten, G.P. Lepage, Phys. Rev. D51 (1995) 1125; D55 (1997) 5853 (E).

- Factorization in perturbative short-distance coeficients and long-distance matrix elements:

$$d\sigma(a+b \to H+X) = \sum_n d\hat{\sigma}(a+b \to Q\overline{Q}\,[n]+X)\,\langle \mathcal{O}^H\,[n]\rangle,$$

  where the sum includes all colour and angular momentum states of the $Q\overline{Q}$ pair, denoted collectively by $n = {}^{2S+1}L_J^{(c)}$.
- Long-distance matrix elements (free parameters) universal, relative sizes predicted by velocity scaling rules.
- Double expansion in α_s and v.
- Renormalizable, predictive.

Introduction

Models for charmonium production

NRQCD factorization formalism:

W. E. Caswell, G. P. Lepage, Phys. Lett. B167 (1986) 437; G.T. Bodwin, E. Braaten, G.P. Lepage, Phys. Rev. D51 (1995) 1125; D55 (1997) 5853 (E).

- Factorization in perturbative short-distance coeficients and long-distance matrix elements:

$$d\sigma(a+b \to H+X) = \sum_n d\hat{\sigma}(a+b \to Q\overline{Q}\,[n]+X)\,\langle \mathcal{O}^H\,[n]\rangle,$$

  where the sum includes all colour and angular momentum states of the $Q\overline{Q}$ pair, denoted collectively by $n = {}^{2S+1}L_J^{(c)}$.
- Long-distance matrix elements (free parameters) universal, relative sizes predicted by velocity scaling rules.
- Double expansion in α_s and υ.
- Renormalizable, predictive.

Introduction

Models for charmonium production

NRQCD factorization formalism:

W. E. Caswell, G. P. Lepage, Phys. Lett. B167 (1986) 437; G.T. Bodwin, E. Braaten, G.P. Lepage, Phys. Rev. D51 (1995) 1125; D55 (1997) 5853 (E).

- Factorization in perturbative short-distance coeficients and long-distance matrix elements:

$$d\sigma(a+b\to H+X)=\sum_n d\hat{\sigma}(a+b\to Q\overline{Q}\,[n]+X)\,\langle\mathcal{O}^H\,[n]\rangle,$$

  where the sum includes all colour and angular momentum states of the $Q\overline{Q}$ pair, denoted collectively by $n={}^{2S+1}L_J^{(c)}$.
- Long-distance matrix elements (free parameters) universal, relative sizes predicted by velocity scaling rules.
- Double expansion in α_s and υ.
- Renormalizable, predictive.

Charmonium production at HERA

The analysis of J/ψ cross sections at HERA provides a powerful tool to assess the importance of the different quarkonium production mechanisms and to test the general picture developed in the context of NRQCD factorization.

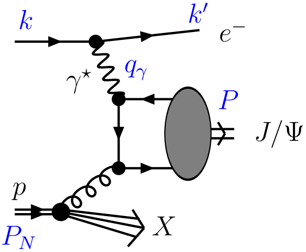

$$S = (P_N + k)^2 = 2P_N k$$

$$Q^2 = -q_\gamma^2 = 2kk'$$

$$y = \frac{P_N q_\gamma}{P_N k}$$

$$\hat{s} = (p + q_\gamma)^2 = xyS - Q^2$$

$$W^2 = (P_N + q_\gamma)^2 = yS - Q^2$$

Charmonium production at HERA

The analysis of J/ψ cross sections at HERA provides a powerful tool to assess the importance of the different quarkonium production mechanisms and to test the general picture developed in the context of NRQCD factorization.

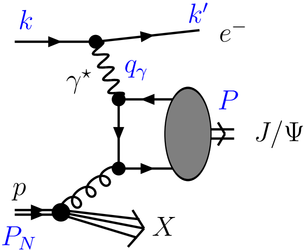

$$S = (P_N + k)^2 = 2P_N k$$

$$Q^2 = -q_\gamma^2 = 2kk'$$

$$y = \frac{P_N q_\gamma}{P_N k}$$

$$\hat{s} = (p + q_\gamma)^2 = xyS - Q^2$$

$$W^2 = (P_N + q_\gamma)^2 = yS - Q^2$$

At the Born level: only color-octet states ${}^1S_0^{(8)}$ and ${}^3P_J^{(8)}$

Charmonium production at HERA

The analysis of J/ψ cross sections at HERA provides a powerful tool to assess the importance of the different quarkonium production mechanisms and to test the general picture developed in the context of NRQCD factorization.

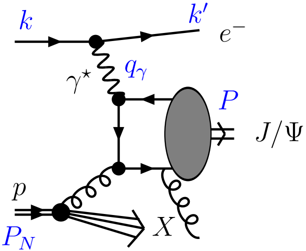

$$S = (P_N + k)^2 = 2P_N k$$

$$Q^2 = -q_\gamma^2 = 2kk'$$

$$y = \frac{P_N q_\gamma}{P_N k}$$

$$\hat{s} = (p + q_\gamma)^2 = xyS - Q^2$$

$$W^2 = (P_N + q_\gamma)^2 = yS - Q^2$$

$$z = \frac{P_N P}{P_N q_\gamma} \overset{p.r.f.}{=} \frac{E_\psi}{E_\gamma}$$

At the Born level: only color-octet states ${}^1S_0^{(8)}$ and ${}^3P_J^{(8)}$

Additional parton in final state: additional variables z, which is defined as the energy fraction, transferred from the photon to the charmonium H in the proton rest frame.

LO results

S. Fleming and T. Mehen, Phys. Rev. D57 (1998) 1846

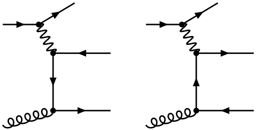

The cross section can be written as:

$$d\sigma(eg \to ec\bar{c}[n]) = \frac{dQ^2 dy}{16\pi x S}\delta(\hat{s} - M^2)\frac{G^2}{Q^4}L_e^{\mu\nu}H_{eg\ \mu\nu}[n]$$

with the leptonic tensor

$$L_e^{\mu\nu} = \frac{Q^2}{y}\left[\frac{1+(1-y)^2}{y}\epsilon_T^{\mu\nu} - \frac{4(1-y)}{y}\epsilon_L^{\mu\nu}\right] ,$$

where

$$\epsilon_T^{\mu\nu} = -g^{\mu\nu} + \frac{1}{pq_\gamma}(p^\mu q_\gamma^\nu + p^\nu q_\gamma^\mu) - \frac{q_\gamma^2}{(pq_\gamma)^2}p^\mu p^\nu ,$$

$$\epsilon_L^{\mu\nu} = \frac{1}{q_\gamma^2}\left(q_\gamma - \frac{q_\gamma^2}{pq_\gamma}p\right)^\mu \left(q_\gamma - \frac{q_\gamma^2}{pq_\gamma}p\right)^\nu .$$

LO results

S. Fleming and T. Mehen, Phys. Rev. D57 (1998) 1846

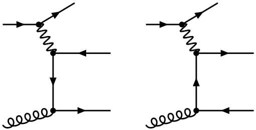

The cross section can be written as:

$$d\sigma(eg \to ec\bar{c}[n]) = \frac{dQ^2 dy}{16\pi x S}\delta(\hat{s} - M^2)\frac{G^2}{Q^4}L_e^{\mu\nu}H_{eg\ \mu\nu}[n]$$

Differential cross-section for $ep \to eHX'$

$$\frac{d\sigma}{dQ^2 dy} = \int_0^1 dx F_N^g(x, \mu_F^2)\delta(xyS - M^2 - Q^2)\frac{8\pi^2 e_c^2 \alpha^2 \alpha_s}{M(M^2+Q^2)Q^2}M_0[n]\frac{\langle O^H[n]\rangle}{N_{\mathrm{col}}N_{\mathrm{pol}}},$$

with

$$M_0\left[{}^1S_0^{(8)}\right] = \frac{1+(1-y)^2}{y}$$

$$M_0\left[{}^3P_0^{(8)}\right] = \frac{1+(1-y)^2}{y}\,\frac{4}{M^2}\,\frac{7M^4+2M^2Q^2+3Q^4}{(M^2+Q^2)^2} + \frac{1-y}{y}\,\frac{64Q^2}{(M^2+Q^2)^2}$$

LO results

S. Fleming and T. Mehen, Phys. Rev. D57 (1998) 1846

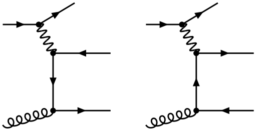

The cross section can be written as:

$$d\sigma(eg \to ec\bar{c}[n]) = \frac{dQ^2 dy}{16\pi x S}\delta(\hat{s} - M^2)\frac{G^2}{Q^4}L_e^{\mu\nu}H_{eg\,\mu\nu}[n]$$

Differential cross-section for $ep \to eHX'$

$$\frac{d\sigma}{dQ^2 dy} = \int_0^1 dx F_N^g(x, \mu_F^2)\delta(xyS - M^2 - Q^2)\frac{8\pi^2 e_c^2 \alpha^2 \alpha_s}{M(M^2+Q^2)Q^2}M_0[n]\frac{\langle O^H[n]\rangle}{N_{\mathrm{col}}N_{\mathrm{pol}}},$$

with

$$M_0\left[{}^1S_0^{(8)}\right] = \frac{1+(1-y)^2}{y}$$

$$M_0\left[{}^3P_0^{(8)}\right] = \frac{1+(1-y)^2}{y}\frac{4}{M^2}\frac{7M^4+2M^2Q^2+3Q^4}{(M^2+Q^2)^2} + \frac{1-y}{y}\frac{64Q^2}{(M^2+Q^2)^2}$$

Large contribution from diffraction and higher twists - can be suppressed with large Q^2

Real corrections

The final state contains additionally a jet j: $ep \to eHjX'$

"J/ψ inclusive production in e p deep-inelastic scattering at DESY HERA,"
B. A. Kniehl and L. Zwirner, Nucl. Phys. B621 (2002) 337

Partonic subprocesses: $eg \to ec\bar{c}[n]g$

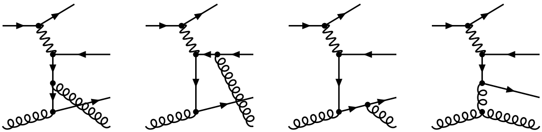

Partonic subprocesses: $eq \to ec\bar{c}[n]q$

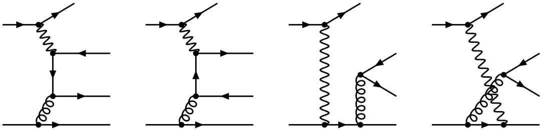

J/ψ energy variable z:
in the proton rest frame, z is the ratio of the J/ψ to γ energy, $z = E_\psi/E_\gamma$.

Real corrections

The final state contains additionally a jet j: $ep \longrightarrow eH\,j\,X'$

"J/ψ inclusive production in e p deep-inelastic scattering at DESY HERA,"
B. A. Kniehl and L. Zwirner, Nucl. Phys. B621 (2002) 337

Partonic subprocesses: $eg \longrightarrow ec\bar{c}[n]g$

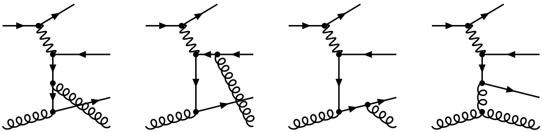

Partonic subprocesses: $eq \longrightarrow ec\bar{c}[n]q$

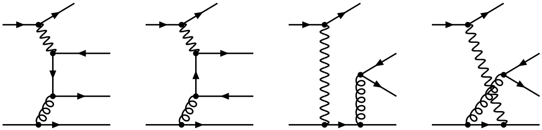

J/ψ energy variable z:
in the proton rest frame, z is the ratio of the J/ψ to γ energy, $z = E_\psi/E_\gamma$.

The real corrections contain infrared and collinear singularities when $z = 1$.

Real corrections

The final state contains additionally a jet j: $ep \longrightarrow eHjX'$

"J/ψ inclusive production in e p deep-inelastic scattering at DESY HERA," B. A. Kniehl and L. Zwirner, Nucl. Phys. B621 (2002) 337

Partonic subprocesses: $eg \longrightarrow ec\bar{c}[n]g$

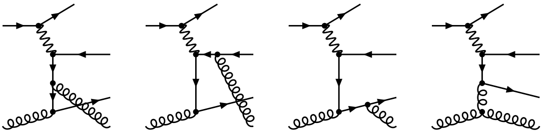

Partonic subprocesses: $eq \longrightarrow ec\bar{c}[n]q$

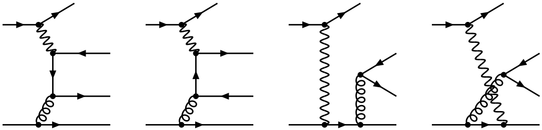

J/ψ energy variable z:
in the proton rest frame, z is the ratio of the J/ψ to γ energy, $z = E_\psi/E_\gamma$.

The real corrections contain infrared and collinear singularities when $z = 1$.
The result is incomplete: should add the virtual corrections.

Virtual corrections

Analytical calculations

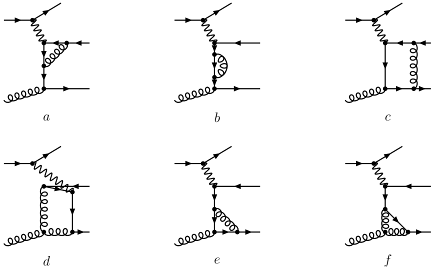

$$
\begin{aligned}
q^2 &= -m^2 \upsilon^2 \\
P^2 &= M^2(1+\upsilon^2) \\
Pq &= 0 \\
pq &= -\frac{\hat{s}+Q^2}{2\sqrt{\hat{s}}} m\, \upsilon \cos\theta
\end{aligned}
$$

Coulomb divergence: is regularized by assigning an infinitesimal velocity υ to the heavy quarks in the quarkonium rest frame. The Coulomb divergent amplitude (diagram c) is not calculated for $q = 0$ but is calculated under consideration of the above identities, where θ is the angle between the momenta $\vec{p}$ and $\vec{q} \equiv m\vec{\upsilon}$ in the quarkonium rest frame.

Virtual corrections
Covariant projection method

A. Petrelli, M. Cacciari, M. Greco, F. Maltoni and M. L. Mangano, Nucl. Phys. B514 (1998) 245

Angular momentum projectors:

$$\mathcal{M}\left[{}^1S_0^{(c)}\right] = tr\left[\mathcal{T}\Pi_0\mathcal{C}_c\right]\Big|_{q_\alpha=0}, \qquad \mathcal{M}\left[{}^3S_1^{(c)}\right] = \epsilon_\alpha\ tr\left[\mathcal{T}\Pi_1^\alpha\mathcal{C}_c\right]\Big|_{q_\alpha=0},$$

$$\mathcal{M}\left[{}^1P_1^{(c)}\right] = \epsilon_\alpha\ \frac{\partial}{\partial q_\alpha} tr\left[\mathcal{T}\Pi_0\mathcal{C}_c\right]\Big|_{q_\alpha=0}, \quad \mathcal{M}\left[{}^3P_J^{(c)}\right] = \mathcal{E}_{\alpha\beta}^{(J)}\ \frac{\partial}{\partial q_\alpha} tr\left[\mathcal{T}\Pi_1^\beta\mathcal{C}_c\right]\Big|_{q_\alpha=0},$$

where $\mathcal{T}$ is the heavy quark spinor amputated Feynman amplitude for the perturbative creation of a heavy quark Q with momentum $p = P/2 + q$ and a heavy antiquark $\bar{Q}$ with momentum $\bar{p} = P/2 - q$ and $q = (p - \bar{p})/2$ in the $Q\bar{Q}$ center of mass system $q_{CMS} = (0, \vec{q}_{CMS})$ with $\vec{q}_{CMS}$ being the nonrelativistic heavy quark momentum.

Spin and color projectors on $Q\bar{Q}$ configurations:

$$\Pi_0 = \frac{1}{\sqrt{8m^3}}\left(\frac{\hat{P}}{2} - \hat{q} - m\right)\gamma_5\left(\frac{\hat{P}}{2} + \hat{q} + m\right), \qquad \mathcal{C}_1 = \frac{\delta_{ij}}{\sqrt{3}},$$

$$\Pi_1^\alpha = \frac{1}{\sqrt{8m^3}}\left(\frac{\hat{P}}{2} - \hat{q} - m\right)\gamma^\alpha\left(\frac{\hat{P}}{2} + \hat{q} + m\right), \qquad \mathcal{C}_8 = \sqrt{2}\,T_{ij}^c.$$

Virtual corrections
Covariant projection method

ϵ_α and $\mathcal{E}^{(J)}_{\alpha\beta}$ are the polarization vector and accordingly the polarization tensor of a $Q\bar{Q}$ configuration with total angular momentum J. ϵ_α and $\mathcal{E}^{(J)}_{\alpha\beta}$ satisfy the polarization sum relations

$$\sum_{J_z=-J}^{J} \epsilon^*_{\alpha'}\epsilon_\alpha = \Pi_{\alpha'\alpha}\,, \qquad \sum_{J_z=-J}^{J} \mathcal{E}^{(J)*}_{\alpha'\beta'}\,\mathcal{E}^{(J)}_{\alpha\beta} = \Pi^{(J)}_{\alpha'\beta'\alpha\beta}$$

with

$$\Pi_{\alpha\beta} = -g_{\alpha\beta} + \frac{P_\alpha P_\beta}{M^2}$$

and

$$\Pi^{(J)}_{\alpha'\beta'\alpha\beta} = \begin{cases} \dfrac{1}{D-1}\Pi_{\alpha'\beta'}\Pi_{\alpha\beta}\,;\ J=0 \\ \dfrac{1}{2}[\Pi_{\alpha'\alpha}\Pi_{\beta'\beta} - \Pi_{\alpha'\beta}\Pi_{\beta'\alpha}]\,;\ J=1 \\ \dfrac{1}{2}[\Pi_{\alpha'\alpha}\Pi_{\beta'\beta} + \Pi_{\alpha'\beta}\Pi_{\beta'\alpha}] - \dfrac{1}{D-1}\Pi_{\alpha'\beta'}\Pi_{\alpha\beta}\,;\ J=2\,. \end{cases}$$

Virtual corrections

Computational details

- Diagram generations and amplitudes: DIANA (QGRAF)
- Reduction of tensor integrals: FeynCalc

  Passarino-Veltman function should be finite in $v \to 0$ limit in spite of the Gramm determinant vanish in this limit.
- Projection, color and Dirac trace, evaluation: FORM
- Simplification: MATHEMATICA

Virtual corrections

Computational details

- Diagram generations and amplitudes: DIANA (QGRAF)
- Reduction of tensor integrals: FeynCalc

  Passarino-Veltman function should be finite in $v \to 0$ limit in spite of the Gramm determinant vanish in this limit.
- Projection, color and Dirac trace, evaluation: FORM
- Simplification: MATHEMATICA

Virtual corrections
Computational details

- Diagram generations and amplitudes: DIANA (QGRAF)
- Reduction of tensor integrals: FeynCalc

  Passarino-Veltman function should be finite in $v \to 0$ limit in spite of the Gramm determinant vanish in this limit.

- Projection, color and Dirac trace, evaluation: FORM
- Simplification: MATHEMATICA

Virtual corrections

Computational details

- Diagram generations and amplitudes: DIANA (QGRAF)
- Reduction of tensor integrals: FeynCalc

  Passarino-Veltman function should be finite in $v \to 0$ limit in spite of the Gramm determinant vanish in this limit.

- Projection, color and Dirac trace, evaluation: FORM
- Simplification: MATHEMATICA

Virtual corrections

Computational details

- Diagram generations and amplitudes: DIANA (QGRAF)
- Reduction of tensor integrals: FeynCalc

  Passarino-Veltman function should be finite in $v \to 0$ limit in spite of the Gramm determinant vanish in this limit.

- Projection, color and Dirac trace, evaluation: FORM
- Simplification: MATHEMATICA

In the limit $Q^2 \to 0$:

$$\frac{d\sigma}{dQ^2dy}(eg \to ec\bar{c}[n])\Big|_{Q^2\to 0} = \frac{\alpha}{2\pi Q^2}\frac{1+(1-y)^2}{y}\sigma(\gamma g \to c\bar{c}[n])$$

Results

UV, IR, collinear and Coulomb divergences

Final result for the virtual corrections reads (after UV renormalization)

$$\frac{\alpha_s}{\pi} M_B \left[\frac{\mathcal{C}\pi^2}{2v} - \frac{3C_\epsilon}{2\epsilon^2} - \frac{3C_\epsilon}{2\epsilon} \left(\frac{51 - 2n_f}{18} - 2\ln\frac{2(M^2+Q^2)}{M^2} \right) \right] + \text{finite terms}$$

- The ultraviolet divergences: the renormalization of the gluon wave function and the strong coupling constant in the $\overline{MS}$ scheme and the heavy quark wave function and mass in the on-shell scheme.
- The infrared and collinear divergences: agree up to the sign with the infrared divergences in the real corrections in accordance with the Kinoshita-Lee-Nauenberg theorem.
- The Coulomb divergence: occurs as factor $1 + \frac{\alpha_s \mathcal{C}\pi}{2v}$, which multiplies M_B and we can factorize it into the $[n]$ production matrix element according to

$$\frac{d\widehat{\widehat{\sigma}}_a}{dQ^2 dy} \left\langle \widehat{O}^{J/\psi}[n] \right\rangle = \frac{d\sigma_a}{dQ^2 dy} \left\langle O^{J/\psi}[n] \right\rangle + o(\alpha^2 \alpha_s^3) \, ,$$

where the redefined $\sigma_g \equiv \sigma\left(eg \to ec\bar{c}[n]g\right)$ is obtained from $\widehat{\widehat{\sigma}}_g$ by deleting the $1/v$ pole term.

Results

UV, IR, collinear and Coulomb divergences

Final result for the virtual corrections reads (after UV renormalization)

$$\frac{\alpha_s}{\pi} M_B \left[\frac{\mathcal{C}\pi^2}{2v} - \frac{3C_\epsilon}{2\epsilon^2} - \frac{3C_\epsilon}{2\epsilon} \left(\frac{51 - 2n_f}{18} - 2\ln\frac{2(M^2+Q^2)}{M^2} \right) \right] + \text{finite terms}$$

- The ultraviolet divergences: the renormalization of the gluon wave function and the strong coupling constant in the $\overline{MS}$ scheme and the heavy quark wave function and mass in the on-shell scheme.
- The infrared and collinear divergences: agree up to the sign with the infrared divergences in the real corrections in accordance with the Kinoshita-Lee-Nauenberg theorem.
- The Coulomb divergence: occurs as factor $1 + \frac{\alpha_s \mathcal{C}\pi}{2v}$, which multiplies M_B and we can factorize it into the $[n]$ production matrix element according to

$$\frac{d\widehat{\widehat{\sigma}}_a}{dQ^2 dy} \left\langle \widehat{O}^{J/\psi}[n] \right\rangle = \frac{d\sigma_a}{dQ^2 dy} \left\langle O^{J/\psi}[n] \right\rangle + o(\alpha^2 \alpha_s^3) \ ,$$

where the redefined $\sigma_g \equiv \sigma\left(eg \to ec\bar{c}[n]g\right)$ is obtained from $\widehat{\widehat{\sigma}}_g$ by deleting the $1/v$ pole term.

Results

UV, IR, collinear and Coulomb divergences

Final result for the virtual corrections reads (after UV renormalization)

$$\frac{\alpha_s}{\pi} M_B \left[\frac{\mathcal{C}\pi^2}{2v} - \frac{3C_\epsilon}{2\epsilon^2} - \frac{3C_\epsilon}{2\epsilon} \left(\frac{51 - 2n_f}{18} - 2\ln\frac{2(M^2+Q^2)}{M^2} \right) \right] + \text{finite terms}$$

- The ultraviolet divergences: the renormalization of the gluon wave function and the strong coupling constant in the $\overline{MS}$ scheme and the heavy quark wave function and mass in the on-shell scheme.
- The infrared and collinear divergences: agree up to the sign with the infrared divergences in the real corrections in accordance with the Kinoshita-Lee-Nauenberg theorem.
- The Coulomb divergence: occurs as factor $1 + \frac{\alpha_s \mathcal{C}\pi}{2v}$, which multiplies M_B and we can factorize it into the $[n]$ production matrix element according to

$$\frac{d\widehat{\widehat{\sigma}}_a}{dQ^2 dy} \left\langle \widehat{O}^{J/\psi}[n] \right\rangle = \frac{d\sigma_a}{dQ^2 dy} \left\langle O^{J/\psi}[n] \right\rangle + o(\alpha^2 \alpha_s^3) \, ,$$

where the redefined $\sigma_g \equiv \sigma\left(eg \to ec\bar{c}[n]g\right)$ is obtained from $\widehat{\widehat{\sigma}}_g$ by deleting the $1/v$ pole term.

Results

UV, IR, collinear and Coulomb divergences

Final result for the virtual corrections reads (after UV renormalization)

$$\frac{\alpha_s}{\pi} M_B \left[\frac{\mathcal{C}\pi^2}{2\upsilon} - \frac{3C_\epsilon}{2\epsilon^2} - \frac{3C_\epsilon}{2\epsilon} \left(\frac{51 - 2n_f}{18} - 2\ln \frac{2(M^2+Q^2)}{M^2} \right) \right] + \text{finite terms}$$

- The ultraviolet divergences: the renormalization of the gluon wave function and the strong coupling constant in the $\overline{MS}$ scheme and the heavy quark wave function and mass in the on-shell scheme.
- The infrared and collinear divergences: agree up to the sign with the infrared divergences in the real corrections in accordance with the Kinoshita-Lee-Nauenberg theorem.
- The Coulomb divergence: occurs as factor $1 + \frac{\alpha_s \mathcal{C}\pi}{2\upsilon}$, which multiplies M_B and we can factorize it into the $[n]$ production matrix element according to

$$\frac{d\widehat{\widehat{\sigma}}_a}{dQ^2 dy} \left\langle \widehat{O}^{J/\psi}[n] \right\rangle = \frac{d\sigma_a}{dQ^2 dy} \left\langle O^{J/\psi}[n] \right\rangle + o(\alpha^2 \alpha_s^3) \ ,$$

where the redefined $\sigma_g \equiv \sigma\left(eg \to ec\bar{c}[n]g\right)$ is obtained from $\widehat{\widehat{\sigma}}_g$ by deleting the $1/\upsilon$ pole term.

Results

Analytical total result

$$\frac{d\sigma\,(eg\to ec\bar{c}[n]g)}{dQ^2dy} = M_0\left\{\left(1+\frac{\alpha_s}{\pi}g[n]\right)\delta(1-x)\right.$$

$$\left.+\frac{\alpha_s}{\pi}\left[\left[\frac{1}{2}\ln\frac{\mu_F^2}{\hat{s}}\left(\frac{1}{1-x}\right)_\rho-\left(\frac{\ln(1-x)}{1-x}\right)_\rho\right](1-x)K_{gg}(x,Q^2)+\left(\frac{1}{1-x}\right)_\rho f_g[n]\right]\right\}$$

with $M_0\,g\left[{}^1S_0^{(8)}\right]=M_0\left[{}^1S_0^{(8)}\right]\hat{T}\left[{}^1S_0^{(8)}\right]$,

$$\hat{T}\left[{}^1S_0^{(8)}\right] = -\frac{1}{2}\left(b_0\ln\frac{{\mu_F}^2}{{\mu_R}^2}-6\left(1+\ln\frac{{\mu_F}^2}{M^2}-l\right)l+12\left(1+\ln\frac{{\mu_F}^2}{M^2}-2\ln(\beta)\right)\ln(\beta)\right)$$

$$+\frac{1}{72}\frac{1}{(M^2+Q^2)(M^2+2Q^2)^2}\Bigg(12(M^2+Q^2)(M^2+2Q^2)(5M^2+18Q^2)-(M^2+2Q^2)^2(3M^2+32Q^2)\pi^2$$

$$-24Q^2(M^2+Q^2)(7M^2+6Q^2)(l+\ln 2)+12(M^2+2Q^2)^2(17M^2+2Q^2)L^2$$

$$-72\sqrt{\frac{Q^2}{M^2+Q^2}}(M^2+2Q^2)(M^2+2Q^2)^2L-12(M^2+2Q^2)^2(9M^2+17Q^2)\mathrm{Li}_2\left(-1-\frac{2Q^2}{M^2}\right)\Bigg),$$

$$b_0 = \frac{11}{2}-\frac{1}{3}n_f,\qquad l=\ln\left(1+\frac{Q^2}{M^2}\right),\qquad L=\ln\left(\frac{\sqrt{Q^2}+\sqrt{M^2+Q^2}}{M}\right).$$

Results

Analytical total result

$$\frac{d\sigma\,(eg \to ec\bar{c}[n]g)}{dQ^2dy} = M_0\Bigg\{\left(1+\frac{\alpha_s}{\pi}g[n]\right)\delta(1-x)$$

$$+\frac{\alpha_s}{\pi}\left[\left[\frac{1}{2}\ln\frac{\mu_F^2}{\hat{s}}\left(\frac{1}{1-x}\right)_\rho-\left(\frac{\ln(1-x)}{1-x}\right)_\rho\right](1-x)K_{gg}(x,Q^2)+\left(\frac{1}{1-x}\right)_\rho f_g[n]\right]\Bigg\}$$

with $M_0\, g\left[{}^1S_0^{(8)}\right] = M_0\left[{}^1S_0^{(8)}\right]\hat{T}\left[{}^1S_0^{(8)}\right]$,

$$\hat{T}\left[{}^1S_0^{(8)}\right] = -\frac{1}{2}\left(b_0\ln\frac{\mu_F{}^2}{\mu_R{}^2}-6\left(1+\ln\frac{\mu_F{}^2}{M^2}-l\right)l+12\left(1+\ln\frac{\mu_F{}^2}{M^2}-2\ln(\beta)\right)\ln(\beta)\right)$$

$$+\frac{1}{72}\frac{1}{(M^2+Q^2)(M^2+2Q^2)^2}\Bigg(12(M^2+Q^2)(M^2+2Q^2)(5M^2+18Q^2)-(M^2+2Q^2)^2(3M^2+32Q^2)\pi^2$$

$$-24Q^2(M^2+Q^2)(7M^2+6Q^2)(l+\ln 2)+12(M^2+2Q^2)^2(17M^2+2Q^2)L^2$$

$$-72\sqrt{\frac{Q^2}{M^2+Q^2}}(M^2+2Q^2)(M^2+2Q^2)^2L-12(M^2+2Q^2)^2(9M^2+17Q^2)\mathrm{Li}_2\left(-1-\frac{2Q^2}{M^2}\right)\Bigg),$$

$$b_0 = \frac{11}{2}-\frac{1}{3}n_f, \qquad l = \ln\left(1+\frac{Q^2}{M^2}\right), \qquad L = \ln\left(\frac{\sqrt{Q^2}+\sqrt{M^2+Q^2}}{M}\right).$$

Agreement in $Q^2 \to 0$ limit diagram by diagram and total with:

"Quarkonium photoproduction at next-to-leading order"
F. Maltoni, M.L. Mangano and A. Petrelli, Nucl. Phys. B519 (1998) 361

Results

Numerical input

- $\sqrt{S} = 318\ GeV$
- $m_c = 1.5 \pm 0.1\ GeV$
- Operator matrix element:

  B. A. Kniehl and C. P. Palisoc, Eur. Phys. J. C48 (2006) 451

$\left\langle \mathcal{O}^{J/\psi}\left[{}^3S_1^{(1)}\right]\right\rangle$	$\left\langle \mathcal{O}^{J/\psi}\left[{}^3S_1^{(8)}\right]\right\rangle$	$M^{J/\psi}_{3.7,3.6}$	$\left\langle \mathcal{O}^{\psi'}\left[{}^3S_1^{(1)}\right]\right\rangle$
1.4 ± 0.1 GeV^3	$(2.3 \pm 0.2) \times 10^{-3}$ GeV^3	$(7.3 \pm 0.2) \times 10^{-2}$ GeV^3	$(6.7 \pm 0.5) \times 10^{-1}$ GeV^3

$\left\langle O^{J/\psi}\left[{}^1S_0^{(8)}\right]\right\rangle = \kappa_{J/\psi} M_r^{J/\psi}$ and $\left\langle O^{J/\psi}\left[{}^3P_0^{(8)}\right]\right\rangle = (1-\kappa_{J/\psi})\frac{m_c^2}{r} M_r^{J/\psi}$

with $r = 3.6$, $\kappa_{J/\psi} = 1/2$

- Proton structure functions: CTEQ6

  J. Pumplin, D. R. Stump, J. Huston, H. L. Lai, P. Nadolsky and W. K. Tung, JHEP0207 (2002) 012

- The renormalization and factorization scale: $\mu_R = \mu_F = \sqrt{M^2 + Q^2}$

Results

Numerical input

- $\sqrt{S} = 318\ GeV$
- $m_c = 1.5 \pm 0.1\ GeV$
- Operator matrix element:

  B. A. Kniehl and C. P. Palisoc, Eur. Phys. J. C48 (2006) 451

$\left\langle \mathcal{O}^{J/\psi}\left[{}^3S_1^{(1)}\right]\right\rangle$	$\left\langle \mathcal{O}^{J/\psi}\left[{}^3S_1^{(8)}\right]\right\rangle$	$M_{3.7,3.6}^{J/\psi}$	$\left\langle \mathcal{O}^{\psi'}\left[{}^3S_1^{(1)}\right]\right\rangle$
1.4 ± 0.1 GeV^3	$(2.3 \pm 0.2) \times 10^{-3}$ GeV^3	$(7.3 \pm 0.2) \times 10^{-2}$ GeV^3	$(6.7 \pm 0.5) \times 10^{-1}$ GeV^3

  $\left\langle O^{J/\psi}\left[{}^1S_0^{(8)}\right]\right\rangle = \kappa_{J/\psi} M_r^{J/\psi}$ and $\left\langle O^{J/\psi}\left[{}^3P_0^{(8)}\right]\right\rangle = (1-\kappa_{J/\psi})\frac{m_c^2}{r} M_r^{J/\psi}$

  with $r = 3.6$, $\kappa_{J/\psi} = 1/2$
- Proton structure functions: CTEQ6

  J. Pumplin, D. R. Stump, J. Huston, H. L. Lai, P. Nadolsky and W. K. Tung, JHEP0207 (2002) 012
- The renormalization and factorization scale: $\mu_R = \mu_F = \sqrt{M^2 + Q^2}$

Results

Numerical input

- $\sqrt{S} = 318\ GeV$
- $m_c = 1.5 \pm 0.1\ GeV$
- Operator matrix element:

  B. A. Kniehl and C. P. Palisoc, Eur. Phys. J. C48 (2006) 451

$\left\langle \mathcal{O}^{J/\psi}\left[{}^3S_1^{(1)}\right]\right\rangle$	$\left\langle \mathcal{O}^{J/\psi}\left[{}^3S_1^{(8)}\right]\right\rangle$	$M^{J/\psi}_{3.7,3.6}$	$\left\langle \mathcal{O}^{\psi'}\left[{}^3S_1^{(1)}\right]\right\rangle$
1.4 ± 0.1 GeV^3	$(2.3 \pm 0.2) \times 10^{-3}$ GeV^3	$(7.3 \pm 0.2) \times 10^{-2}$ GeV^3	$(6.7 \pm 0.5) \times 10^{-1}$ GeV^3

$\left\langle O^{J/\psi}\left[{}^1S_0^{(8)}\right]\right\rangle = \kappa_{J/\psi} M_r^{J/\psi}$ and $\left\langle O^{J/\psi}\left[{}^3P_0^{(8)}\right]\right\rangle = (1-\kappa_{J/\psi})\frac{m_c^2}{r} M_r^{J/\psi}$

with $r = 3.6$, $\kappa_{J/\psi} = 1/2$

- Proton structure functions: CTEQ6

  J. Pumplin, D. R. Stump, J. Huston, H. L. Lai, P. Nadolsky and W. K. Tung, JHEP0207 (2002) 012

- The renormalization and factorization scale: $\mu_R = \mu_F = \sqrt{M^2 + Q^2}$

Results
Numerical input

- $\sqrt{S} = 318\ GeV$
- $m_c = 1.5 \pm 0.1\ GeV$
- Operator matrix element:

  B. A. Kniehl and C. P. Palisoc, Eur. Phys. J. C48 (2006) 451

$\left\langle \mathcal{O}^{J/\psi}\left[{}^3S_1^{(1)}\right]\right\rangle$	$\left\langle \mathcal{O}^{J/\psi}\left[{}^3S_1^{(8)}\right]\right\rangle$	$M^{J/\psi}_{3.7,3.6}$	$\left\langle \mathcal{O}^{\psi'}\left[{}^3S_1^{(1)}\right]\right\rangle$
1.4 ± 0.1 GeV^3	$(2.3 \pm 0.2) \times 10^{-3}$ GeV^3	$(7.3 \pm 0.2) \times 10^{-2}$ GeV^3	$(6.7 \pm 0.5) \times 10^{-1}$ GeV^3

$$\left\langle O^{J/\psi}\left[{}^1S_0^{(8)}\right]\right\rangle = \kappa_{J/\psi} M_r^{J/\psi} \text{ and } \left\langle O^{J/\psi}\left[{}^3P_0^{(8)}\right]\right\rangle = (1-\kappa_{J/\psi})\frac{m_c^2}{r} M_r^{J/\psi}$$

  with $r = 3.6$, $\kappa_{J/\psi} = 1/2$

- Proton structure functions: CTEQ6

  J. Pumplin, D. R. Stump, J. Huston, H. L. Lai, P. Nadolsky and W. K. Tung, JHEP0207 (2002) 012

- The renormalization and factorization scale: $\mu_R = \mu_F = \sqrt{M^2 + Q^2}$

Results

Numerical input

- $\sqrt{S} = 318\ GeV$
- $m_c = 1.5 \pm 0.1\ GeV$
- Operator matrix element:

  B. A. Kniehl and C. P. Palisoc, Eur. Phys. J. C48 (2006) 451

$\left\langle \mathcal{O}^{J/\psi}\left[{}^3S_1^{(1)}\right]\right\rangle$	$\left\langle \mathcal{O}^{J/\psi}\left[{}^3S_1^{(8)}\right]\right\rangle$	$M^{J/\psi}_{3.7,3.6}$	$\left\langle \mathcal{O}^{\psi'}\left[{}^3S_1^{(1)}\right]\right\rangle$
1.4 ± 0.1 GeV^3	$(2.3 \pm 0.2) \times 10^{-3}$ GeV^3	$(7.3 \pm 0.2) \times 10^{-2}$ GeV^3	$(6.7 \pm 0.5) \times 10^{-1}$ GeV^3

  $\left\langle O^{J/\psi}\left[{}^1S_0^{(8)}\right]\right\rangle = \kappa_{J/\psi} M_r^{J/\psi}$ and $\left\langle O^{J/\psi}\left[{}^3P_0^{(8)}\right]\right\rangle = (1-\kappa_{J/\psi})\frac{m_c^2}{r} M_r^{J/\psi}$

  with $r = 3.6$, $\kappa_{J/\psi} = 1/2$
- Proton structure functions: CTEQ6

  J. Pumplin, D. R. Stump, J. Huston, H. L. Lai, P. Nadolsky and W. K. Tung, JHEP0207 (2002) 012
- The renormalization and factorization scale: $\mu_R = \mu_F = \sqrt{M^2 + Q^2}$

Results
Numerical input

- $\sqrt{S} = 318\ GeV$
- $m_c = 1.5 \pm 0.1\ GeV$
- Operator matrix element:

  B. A. Kniehl and C. P. Palisoc, Eur. Phys. J. C48 (2006) 451

$\left\langle \mathcal{O}^{J/\psi}\left[{}^3S_1^{(1)}\right]\right\rangle$	$\left\langle \mathcal{O}^{J/\psi}\left[{}^3S_1^{(8)}\right]\right\rangle$	$M^{J/\psi}_{3.7,3.6}$	$\left\langle \mathcal{O}^{\psi'}\left[{}^3S_1^{(1)}\right]\right\rangle$
1.4 ± 0.1 GeV^3	$(2.3 \pm 0.2) \times 10^{-3}$ GeV^3	$(7.3 \pm 0.2) \times 10^{-2}$ GeV^3	$(6.7 \pm 0.5) \times 10^{-1}$ GeV^3

  $\left\langle O^{J/\psi}\left[{}^1S_0^{(8)}\right]\right\rangle = \kappa_{J/\psi} M_r^{J/\psi}$ and $\left\langle O^{J/\psi}\left[{}^3P_0^{(8)}\right]\right\rangle = (1-\kappa_{J/\psi})\frac{m_c^2}{r} M_r^{J/\psi}$

  with $r = 3.6$, $\kappa_{J/\psi} = 1/2$
- Proton structure functions: CTEQ6

  J. Pumplin, D. R. Stump, J. Huston, H. L. Lai, P. Nadolsky and W. K. Tung, JHEP0207 (2002) 012
- The renormalization and factorization scale: $\mu_R = \mu_F = \sqrt{M^2 + Q^2}$

Agreement numerically in $Q^2 \to 0$ limit with:

"Quarkonium photoproduction at next-to-leading order"
F. Maltoni, M.L. Mangano and A. Petrelli, Nucl. Phys. B519 (1998) 361

Results

Q^2-distribution

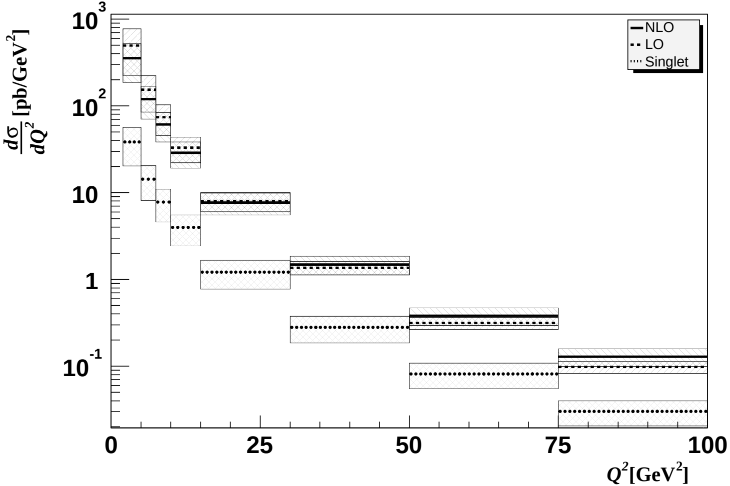

Results

z-distribution

Inclusive production $ep \to eHjX'$:

$$\sigma = \int_{z_{i_{min}}}^{z_{i_{max}}} dz \frac{d\sigma}{dz}$$

B. A. Kniehl and L. Zwirner, Nucl. Phys. B621 (2002) 337

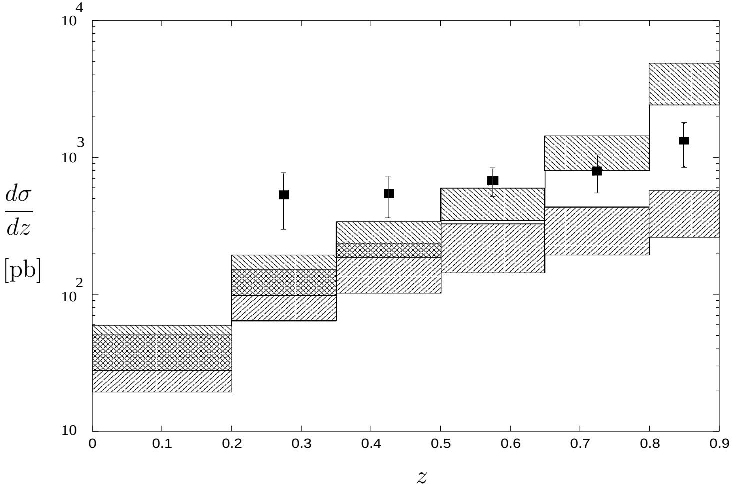

Results

z-distribution

$$\sigma(z > z_{min}) = \int_{z_{min}}^{1} dz \frac{d\sigma}{dz} = \int_0^1 dz \frac{d\sigma}{dz} - \int_0^{z_{min}} dz \frac{d\sigma}{dz}$$

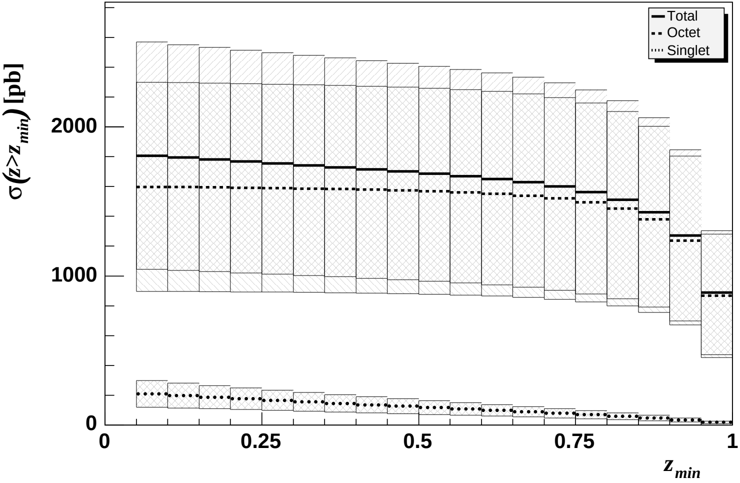

Conclusion

- The NRQCD factorization approach provides a systematic method for calculating quarkonium production rates as a double expansion in powers of α_s and v
- Our complete NLO results for the leptoproduction of J/ψ show the importance of the color-octet contribution in DIS at HERA
- Next step: similar calculations for the polarized case

Conclusion

- The NRQCD factorization approach provides a systematic method for calculating quarkonium production rates as a double expansion in powers of α_s and v
- Our complete NLO results for the leptoproduction of J/ψ show the importance of the color-octet contribution in DIS at HERA
- Next step: similar calculations for the polarized case

Conclusion

- The NRQCD factorization approach provides a systematic method for calculating quarkonium production rates as a double expansion in powers of α_s and v
- Our complete NLO results for the leptoproduction of J/ψ show the importance of the color-octet contribution in DIS at HERA
- Next step: similar calculations for the polarized case